



Insights into the catalysis of a lysine-tryptophan bond in bacterial peptides by a SPASM domain radical S-adenosylmethionine (SAM) peptide cyclase

Received for publication, February 27, 2017, and in revised form, April 26, 2017. Published, Papers in Press, May 5, 2017, DOI 10.1074/jbc.M117.783464

Alhosna Benjdia^{†1}, Laure Decamps[‡], Alain Guillot[‡], Xavier Kubiak[‡], Pauline Ruffié[‡], Corine Sandström[§], and Olivier Berteau^{‡2}

From the [†]Micalis Institute, ChemSyBio, INRA, AgroParisTech, Université Paris-Saclay, 78350 Jouy-en-Josas, France and the [§]Department of Molecular Sciences, Uppsala BioCenter, Swedish University of Agricultural Sciences, P. O. Box 7015, Uppsala 750-07, Sweden

Edited by F. Peter Guengerich

Radical S-adenosylmethionine (SAM) enzymes are emerging as a major superfamily of biological catalysts involved in the biosynthesis of the broad family of bioactive peptides called ribosomally synthesized and post-translationally modified peptides (RiPPs). These enzymes have been shown to catalyze unconventional reactions, such as methyl transfer to electrophilic carbon atoms, sulfur to C_α atom thioether bonds, or carbon-carbon bond formation. Recently, a novel radical SAM enzyme catalyzing the formation of a lysine-tryptophan bond has been identified in *Streptococcus thermophilus*, and a reaction mechanism has been proposed. By combining site-directed mutagenesis, biochemical assays, and spectroscopic analyses, we show here that this enzyme, belonging to the emerging family of SPASM domain radical SAM enzymes, likely contains three [4Fe-4S] clusters. Notably, our data support that the seven conserved cysteine residues, present within the SPASM domain, are critical for enzyme activity. In addition, we uncovered the minimum substrate requirements and demonstrate that KW cyclic peptides are more widespread than anticipated, notably in pathogenic bacteria. Finally, we show a strict specificity of the enzyme for lysine and tryptophan residues and the dependence of an eight-amino acid leader peptide for activity. Altogether, our study suggests novel mechanistic links among SPASM domain radical SAM enzymes and supports the involvement of non-cysteinylligands in the coordination of auxiliary clusters.

Radical SAM enzymes constitute one of the most diverse and versatile superfamily of enzymes, with more than 220,000 enzymes involved in at least 85 biochemical transformations (1–3). These enzymes catalyze chemically challenging reactions, some of which have no counterparts in biology or synthetic chemistry (1, 4). Recently, they have been shown to be key catalysts in the biosynthesis of the broad family of natural products called ribosomally synthesized and post-translationally

modified peptides (RiPPs).³ RiPPs encompass major and diverse families of antibiotics and bacterial toxins, such as lantibiotics, thiopeptides, sactipeptides, and proteusins (5). In the last five years, radical SAM enzymes have been shown to catalyze unique post-translational modifications on RiPPs, such as C_α-thioether (6, 7), carbon-carbon bond formation (8, 34), and various methyl transfer reactions on RiPPs (9, 10).

Interestingly, several of these post-translational modifications are catalyzed by structurally related radical SAM enzymes belonging to the so-called “SPASM domain” group. Initially this group was named for subilimosin, PQQ, anaerobic sulfatases, and mycofactocin (11, 12), the products of the reactions catalyzed by the respective enzymes Alba (6, 7), PqqE (13), anaerobic sulfatase-maturing enzyme (anSME) (14–16), and MftC (17). AnSME is the founding member of the SPASM domain radical SAM enzyme family. It has been shown to catalyze the post-translational modification of a critical serine or cysteine residue into a C_α-formylglycine, required for the activity of the so-called aryl sulfatases (3, 11, 14, 15, 18–21) (Fig. 1). After some controversy, it has been established that anSME, in addition of the radical SAM [4Fe-4S] cluster, contains two auxiliary [4Fe-4S] clusters in the SPASM domain (11, 20). These two [4Fe-4S] clusters are fully coordinated by eight cysteine residues, conserved in all anSME homologs (15, 19, 20, 22).

The second SPASM domain radical SAM enzyme characterized was Alba. Alba catalyzes the formation of C_α-S bonds in the antibacterial peptide subilimosin A (Fig. 1) (6, 7). Intriguingly, this enzyme has seven cysteine residues in its SPASM domain that are conserved with anSME. A recent study pointed out that they are likely involved in the coordination of two auxiliary [4Fe-4S] clusters and that they are required for enzyme activity (6). More recently, PqqE has been shown to catalyze the formation of a C–C bond between a glutamate and a tyrosine residue during the biosynthesis of pyrroloquinoline quinone (13). An early study proposed that PqqE contains a single [4Fe-4S] cluster in its SPASM domain (23). However, similarly to Alba (6), it is now suggested that PqqE possesses two auxiliary

This work was supported in part by European Research Council Consolidator Grant 617053 (to O. B.). The authors declare that they have no conflicts of interest with the contents of this article.

✂ Author's Choice—Final version free via Creative Commons CC-BY license. This article contains supplemental Figs. S1–S9 and Tables S1–S4.

¹ To whom correspondence may be addressed. Tel.: 33-1-34-65-23-08; Fax: 33-1-34-65-24-62; E-mail: Alhosna.Benjdia@inra.fr.

² To whom correspondence may be addressed. E-mail: Olivier.Berteau@inra.fr.

³ The abbreviations used are: RiPP, ribosomally synthesized and post-translationally modified peptide; SPASM, subilimosin, PQQ, anaerobic sulfatases, and mycofactocin; SAM, S-adenosylmethionine; TOCSY, total correlation spectroscopy; HSQC, heteronuclear single quantum coherence; HMBC, heteronuclear multiple bond correlation.

Catalysis of C–C bond by a SPASM domain radical SAM enzyme

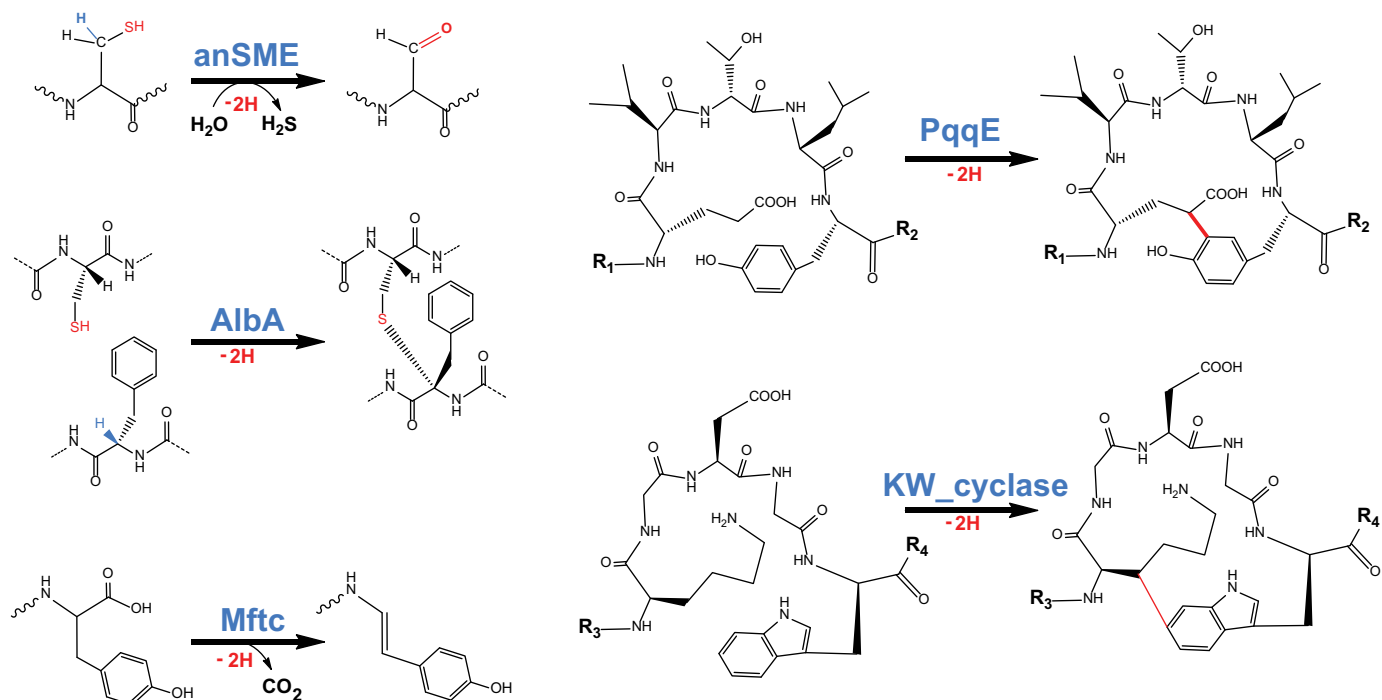


Figure 1. Reactions catalyzed by SPASM domain radical SAM enzymes. Shown are anSME (cysteine or serine oxidation into C_{α} -formylglycine), AlbA (thioether bond formation), MftC (oxidative decarboxylation), PqqE (C–C bond formation), and KW_cyclase (C–C bond formation).

[4Fe-4S] clusters (13), likely coordinated by seven cysteine residues. Finally, recent investigations of MftC (mycofactocin biosynthesis), the “last” SPASM domain radical SAM enzyme, showed that it catalyzes tyrosine decarboxylation (17). However, its mechanism and number of [4Fe-4S] clusters are currently unclear.

All of these enzymes catalyze related reactions (Fig. 1) and have in common that they possess, in their C-terminal region, a SPASM domain that contains [4Fe-4S] clusters. However, the nature, number, and function of these metallic centers are still not well understood (21). Investigated recently, these enzymes appear now to constitute one of the largest groups in the superfamily of radical SAM enzymes. It is thus not surprising that novel SPASM domain radical SAM enzymes are regularly identified.

Recently, the KW_cyclase from *Streptococcus thermophilus* has been shown to catalyze C–C bond formation between a lysine and a tryptophan residue during the biosynthesis of a unique cyclic peptide with unknown function (8, 24). Here we investigated the substrate specificity and the role of conserved cysteine residues in the KW_cyclase from *S. thermophilus* to gain further insights into its mechanism and the large family of SPASM domain radical SAM enzymes.

Results

Substrate specificity of the KW_cyclase

The nucleotide sequence coding for the KW_cyclase of *S. thermophilus* was optimized for expression in *Escherichia coli* and the protein expressed as a Strep-tag fusion protein (Fig. 2a). As shown (Fig. 2b), the purified enzyme exhibited absorption bands at ~ 320 and ~ 410 nm after anaerobic iron-sulfur cluster reconstitution and an A_{420}/A_{280} ratio of ~ 0.3 , similar to

what has been reported for anSME, a radical SAM enzyme containing three [4Fe-4S] clusters (15). Iron-sulfur quantification showed that the KW_cyclase contained 11.8 ± 0.3 mol of iron and 13.6 ± 0.8 mol of sulfide per polypeptide. Collectively, these data support the presence of up to three [4Fe-4S] clusters in the enzyme.

The activity of the KW_cyclase was first assayed with a peptide encompassing the 30-amino acid residues (called here ME_30; Fig. 2c) encoded by the *ster_1357* gene, as reported recently (8). Incubation of the ME_30 peptide in the presence of SAM and sodium dithionite led to the reductive cleavage of SAM into 5'-dA (retention time, 11.3 min, Fig. 2d) and the formation of a peptide product (ME_30*; retention time, 30.4 min; Fig. 2e). MS analysis of this novel peptide ($[M+H]^+$, 3310.3) indicated a mass loss of -2 Da compared with the substrate ($[M+H]^+$, 3312.3; Fig. 2f). This result, implying the loss of two H atoms, was consistent with the activity of the enzyme as a peptide cyclase. LC/MS fragmentation of tryptic peptides confirmed the formation of a bond between the expected amino acid residues: Lys-16 and Trp-20, as demonstrated by the characteristic ions y_6-2 and b_{13} (Fig. 2g and supplemental Figs. S1 and S2 and Tables S1–S3).

To assess whether this enzyme can tolerate amino acid substitution, we synthesized three peptide variants in which we substituted the residues Lys-16 and Trp-20 involved in the formation of the K-W bridge (Fig. 2c). The KW_cyclase has been shown to abstract one lysine C_{β} H atom, generating a carbon-centered radical that is likely to perform a radical addition to the indole ring of tryptophan. We thus substituted Lys-16 with an alanine residue (peptide ME_30AW) or Trp-20 with a phenylalanine (peptide ME_30KF). Finally, as a control, we synthesized a substrate in which Trp-20 was substituted with an ala-

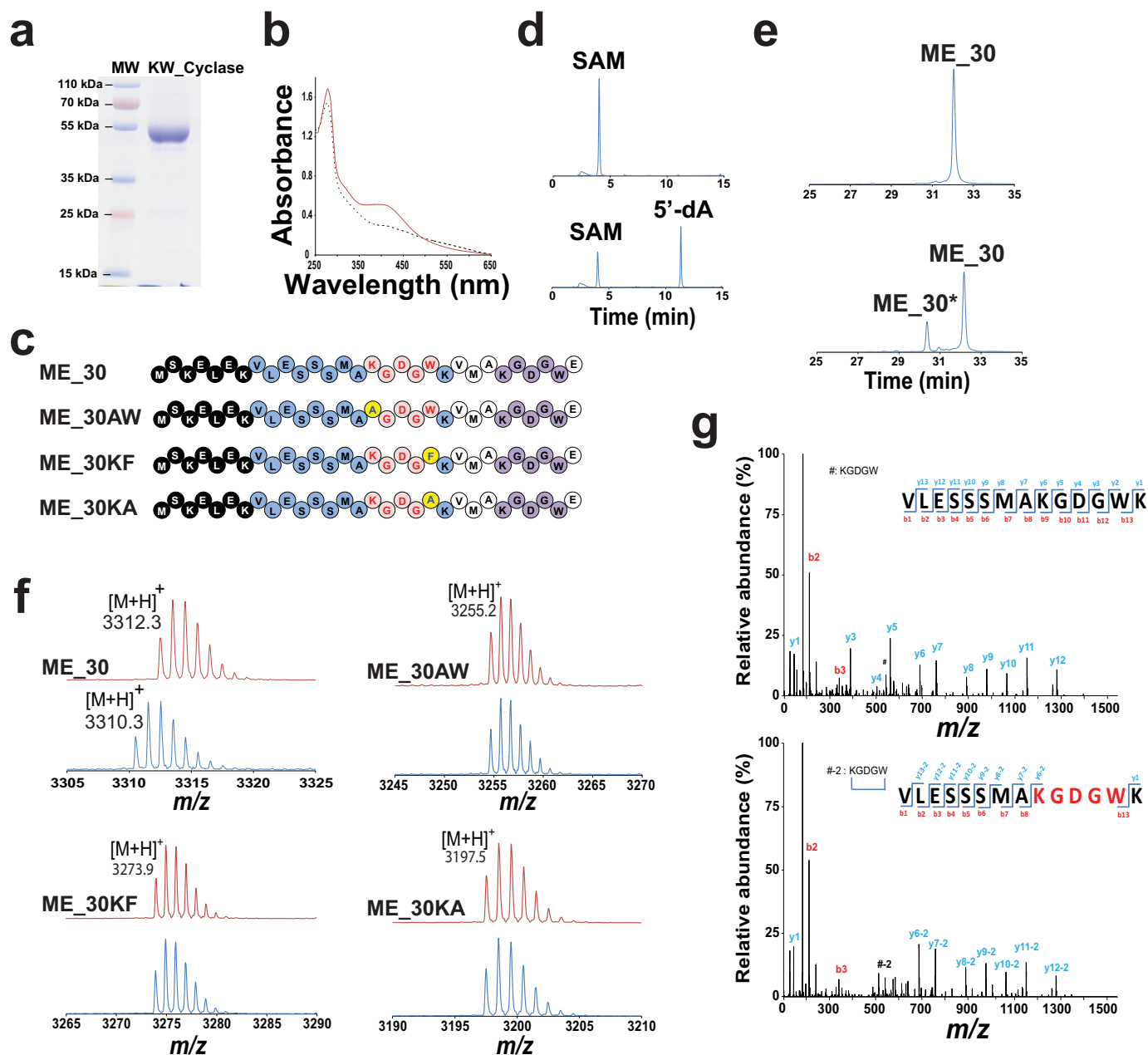


Figure 2. Specificity of the KW_cyclase. *a*, gel electrophoresis analysis (SDS-PAGE, 12.5%) of the purified KW_cyclase. MW, molecular weight. *b*, UV-visible spectrum of KW_cyclase before (16 μ M, dashed line) and after (18 μ M, solid line) anaerobic reconstitution of the [Fe-S] clusters. *c*, sequences of the ME_30, ME_30AW, ME_30KF, and ME_30KA peptides. Black circles correspond to the putative peptide leader based on the alignment in Fig. 3a. The conserved residues are depicted as blue circles. Red circles indicate the residues that form the cyclic KGDGW peptide. The second KGDGW motif is depicted as purple circles. Mutated residues are indicated by a yellow circle. *d*, HPLC analysis of the reductive cleavage of SAM at time 0 (top trace) and after 180-min incubation with KW_cyclase (bottom trace) (see below for experimental conditions). Detection was performed at 257 nm, and 5'-dA was further analyzed by MS. *e*, HPLC analysis of the ME_30 peptide before (top trace) and after 180-min incubation with the KW_cyclase (bottom trace). Detection was performed at 280 nm (see below for experimental conditions). *f*, MALDI-TOF MS analysis of the various peptides used as substrate before (top red traces) and after (bottom blue traces) incubation with KW_cyclase. Reactions were performed by incubating the reconstituted KW_cyclase (50 μ M) with peptide (1 mM), SAM (1 mM), DTT (3 mM), and sodium dithionite (2 mM) under anaerobic conditions. *g*, LC/MS-MS analysis of the ME_30 peptide before (top trace) and after (bottom trace) incubation with KW_cyclase.

nine residue (peptide ME_30KA) to prevent the radical addition of the carbon-centered radical intermediate (Fig. 2c). However, in all of these peptides, we conserved the second KGDGW motif present at the C-terminal end of the ME_30 peptide.

Incubation of each of these peptides with the KW_Cyclase led to efficient reductive cleavage of SAM; nevertheless, HPLC and mass spectrometry analyses failed to show any peptide

modification, even after an extended incubation time (Fig. 2f). The absence of activity on ME_30AW and ME_30KF showed that the enzyme exhibits a strict specificity for the two amino acid residues involved in the formation of the C–C bond. This result is in contrast with the SPASM domain radical SAM enzymes anSME, AlbA, and SkfB, which tolerated amino acid substitutions in their respective substrates (7, 19, 25). Interestingly, substitution of tryptophan with a phenylalanine residue

Catalysis of C–C bond by a SPASM domain radical SAM enzyme

also hindered the reaction despite the fact that, following H atom abstraction, radical addition has been postulated to occur on the benzene ring of tryptophan. Hence, the enzyme appears strictly specific to the Lys and Trp residues and of the relative location of the KGDGW motif in the sequence. Indeed, despite the presence of a second KGDGW motif in the peptides assayed (*purple sequence*, Fig. 2c), this second motif was never modified.

Identification of the minimum KW_cyclase peptide substrate

To further explore the enzyme specificity, we searched for genes encoding homologs of the ME₃₀ peptide in sequenced genomes. Genes encoding peptides are notoriously difficult to predict. Hence, we used the KW_cyclase as a probe and searched for putative peptide-coding genes in the vicinity of the gene coding for the KW_cyclase. Using a cutoff E value of E^{-58} , we identified putative KW_cyclases in the genomes of several other *Streptococcus* species (*Streptococcus salivarius*, *Streptococcus agalactiae*, *Streptococcus suis*, and *Streptococcus mitis*) and in *Lactococcus lactis* as reported previously but also in *Pseudomonas putida*. Interestingly, below this E value, the next homologs retrieved were annotated as PqqE, with the authentic PqqE enzyme from *Klebsiella* among them (E value, E^{-14}) (23).

A search in the upstream region of these radical SAM enzymes led to the identification of small ORFs coding for putative peptides containing the KGDGW motif (Fig. 3a), whereas, in the downstream regions, we identified genes coding for a putative protease and ABC transporter, similar to the *S. thermophilus* operon. Sequence alignment between these putative peptides led to the identification of a minimal consensus peptide containing residues 1–21 with a core region encompassing residues 8–21. Previous attempts to assay the KW_cyclase with peptides shorter than the ME₃₀ peptide failed to identify suitable substrates, suggesting that the whole sequence is important for interaction or activity (8).

To verify this hypothesis, we synthesized a peptide containing the strictly conserved residues 1–21 (peptide MK₂₁) (Fig. 3b). Surprisingly, this sequence, which corresponds to the sequence identified notably in the human pathogen *S. agalactiae*, proved to be an efficient enzyme substrate (Fig. 3, b and c). Indeed, with this shorter substrate ($[M+H]^+$, 2339.7), a new product ($[M+H]^+$, 2337.5) consistent with cyclization activity was formed. To ensure the nature of the product formed, we characterized this peptide by NMR spectroscopy (supplemental Figs. S3–S7). After trypsin digestion, the peptide containing residues 8–21, including the KGDGW motif, was purified by HPLC. The ¹H and ¹³C NMR signals of the constituent amino acids were assigned using a combination of 2D NMR experiments, including COSY, TOCSY, NOESY, HSQC, HMBC, and HSQC-TOCSY (supplemental Figs. S3–S7 and Table S4). The amino acid sequence of the peptide was confirmed by sequential assignment using the $d\alpha N(i, i+1)$ NOE connectivities. Comparison of the TOCSY and HSQC spectra of the linear and cyclic peptide showed that the spin system of Lys-9 (corresponding to Lys-16 in the full-length peptide) was strongly modified. The H_α proton of Lys-9 was shifted downfield by 0.4 ppm and appeared as a doublet instead of a triplet, indicating abstraction of a proton from the carbon-β. The ³J_{αβ} value of 11 Hz suggested a restricted rotation around the C_α-C_β bond with

an HCCH torsion angle of around 180°. In the COSY spectrum, H_α(Lys-9) showed a cross-peak to a signal at 3.5 ppm assigned as H_β(Lys-9), thus deshielded by approximately 1.8 ppm compared with H_β(Lys-14) (corresponding to Lys-21 in the full-length peptide). C_β(Lys-9) was also deshielded by 10 ppm compared with C_β(Lys-14), and the multiplicity-edited HSQC revealed that C_β(Lys-9) was a methine and not a methylene carbon, demonstrating abstraction of a proton at this position. The ¹H NMR spectra and the HSQC spectra of the aromatic region of tryptophan showed only four signals corresponding to four CH groups instead of the five normally observed for unsubstituted tryptophan. This demonstrates abstraction of one proton on one of the carbons of the benzene ring. Analysis of the spin system showed that the C6 proton on the benzene ring appeared as a doublet (instead of a triplet in tryptophan), and this, together with the HMBC spectrum, showed that abstraction occurred at C7 on the six-membered ring. Cyclization was confirmed based on the observation of a diagnostic NOE between H_α of Lys-9 and C6 of Trp and between NH-1 of the tryptophan ring at 10.42 ppm and H_β of Lys-9 at 3.57 ppm. Thus, NMR analysis unambiguously established that, using this shorter substrate, the expected C_β-C7 bond between lysine and tryptophan was formed as found in the peptide naturally produced by *S. thermophilus* (8).

It has been shown recently, in the case of AlbA (6) or PoyC (9), two radical SAM enzymes catalyzing peptide modification, that the leader peptide was dispensable for activity. To test the importance of the leader sequence, we synthesized a novel substrate deprived of the first seven amino acids, which define a conserved sequence in the N-terminal region (Fig. 3a). This novel peptide containing residues 8–21 (peptide VK₁₄, $[M+H]^+$, 1494.0) proved to be an enzyme substrate, albeit with a very low amount of cyclic peptide produced (<1%; $[M+H]^+$, 1491.9; Fig. 3c). The MK₂₁ peptide thus appears to be the minimal substrate for efficient enzyme activity. This result supports a strong dependence of the KW_cyclase to the leader sequence. Kinetic experiments, performed in the presence of the ME₃₀ or MK₂₁ peptide, showed that the production of cyclized peptide and 5'-dA is faster in the presence of the latter peptide, with a k_{cat} of $0.09 \pm 0.005 \text{ min}^{-1}$ and $0.14 \pm 0.01 \text{ min}^{-1}$, respectively (Fig. 3, d and e). Interestingly, with both substrates, we measured a good correlation between the productions of 5'-dA and cyclized peptides, supporting that 1 mole of SAM is consumed per catalytic cycle.

Iron-sulfur clusters of the KW_cyclase

As described above, iron and sulfur quantifications support that the KW_cyclase contains up to three [4Fe-4S] clusters, contrary to previous reports. Among the 13 cysteine residues present in the sequence of the enzyme, Cys-409 and Cys-415 have been mutated previously and proposed, by homology with anSME, to be involved in the coordination of a SPASM domain [4Fe-4S] cluster. The structural analysis of anSME (20) has revealed that four cysteine residues, Cys-317, Cys-320, Cys-326, and Cys-348, coordinate one [4Fe-4S] cluster (called auxiliary II), with the residues Cys-320 and Cys-326 being the equivalent of Cys-409 and Cys-415 in the KW_cyclase (11, 15, 19–21) (Fig. 4a). However, in anSME a second [4Fe-4S] cluster

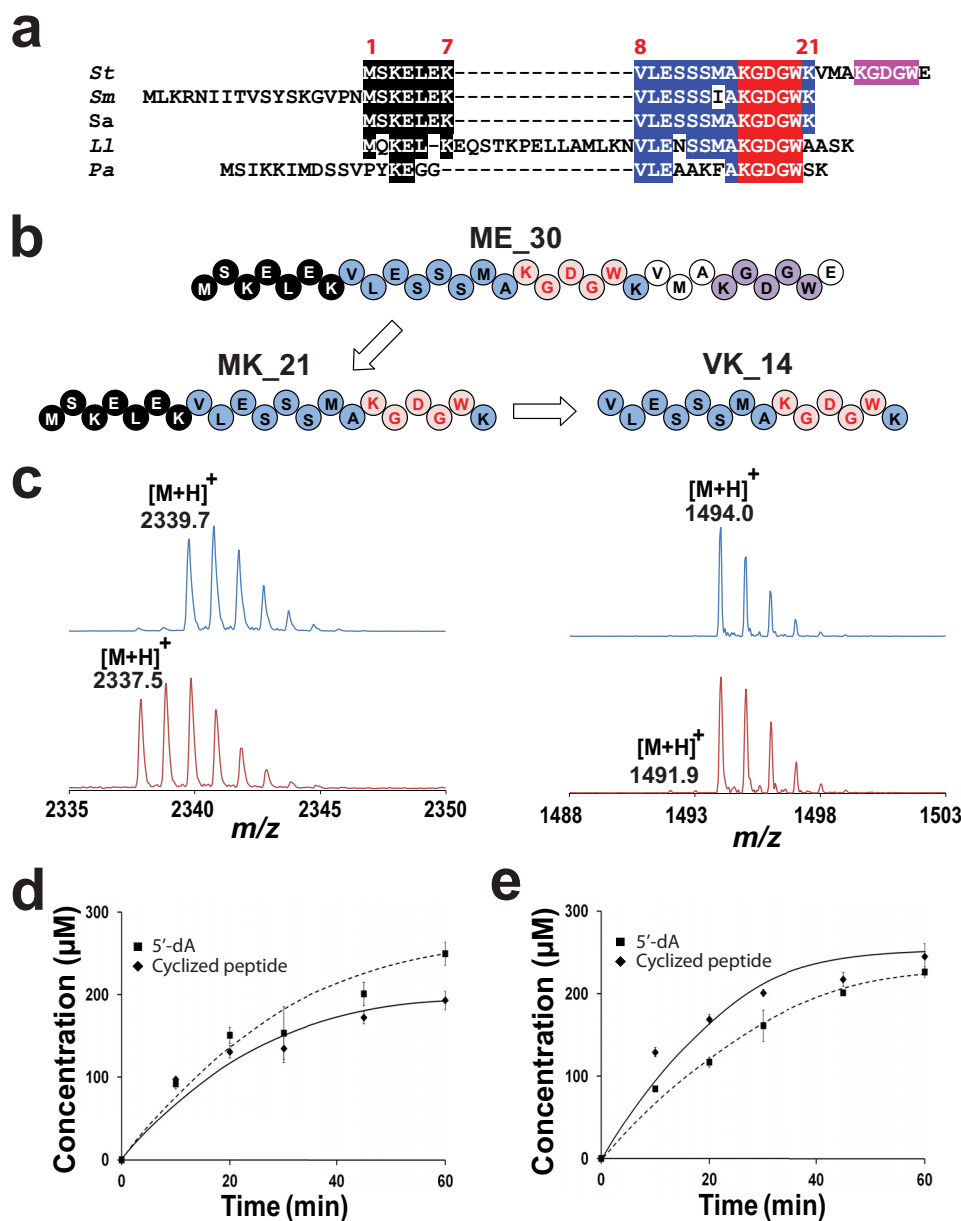


Figure 3. Minimal substrate for KW_cyclase. *a*, sequence alignment of ME_30 peptide homologs found in various bacteria. The putative peptide leader sequence is highlighted in black. The conserved residues are highlighted in blue, whereas the residues involved in the cyclic KGDGW peptide are highlighted in red. The second KGDGW motif, found in *S. thermophilus* is highlighted in purple. *St*, *S. thermophilus*; *Sm*, *S. mitis*; *Sa*, *S. agalactiae*; *Ll*, *L. lactis*; *Pa*, *P. aeruginosa*. *b*, sequences of the ME_30, MK_21, and VK_14 peptides. *c*, MALDI-TOF MS analysis of MK_21 (left panel) and VK_14 (right panel) peptides before (top traces) or after (bottom traces) incubation with KW_cyclase (see below for experimental conditions). *d*, kinetic analysis of the reaction catalyzed by KW_cyclase in the presence of the ME_30 peptide. The data represent the mean \pm S.D. of three independent reactions. See below for experimental conditions. *e*, kinetic analysis of the reaction catalyzed by KW_cyclase in the presence of the MK_21 peptide. Reactions were performed by incubating the reconstituted KW_cyclase (68 μ M) with peptide substrate (1 mM), SAM (1 mM), DTT (3 mM), and sodium dithionite (2 mM) under anaerobic conditions. The data represent the mean \pm S.D. of three independent reactions.

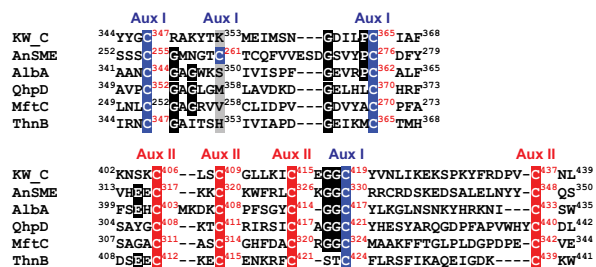
was also identified, buried within the enzyme structure and coordinated by four additional cysteine residues: Cys-255, Cys-261, Cys-276, and Cys-330. This last cluster, close to the radical SAM cluster, was labeled auxiliary I.

Sequence alignment of the KW_cyclase with five biochemically characterized SPASM domain radical SAM enzymes (anSME, AlbA, QhpD, MftC, and ThnB), showed clear conservation of the four cysteine residues involved in the coordination of the auxiliary cluster II (Fig. 4a). Strikingly, all the SPASM domain radical SAM enzymes also possess three conserved cys-

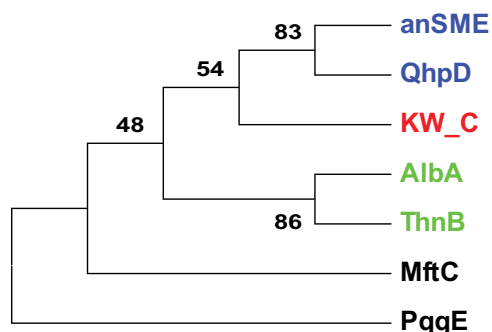
teine residues of the four involved in the coordination of the auxiliary cluster I in anSME (Fig. 4a). In addition, despite these enzymes having no significant homology (identity ranging between 16–26%), it is always the same cysteine residue (Cys-261 in anSME) that is substituted. Of note, this residue is often replaced by residues known to be involved in the coordination of [4Fe-4S] clusters such as serine, histidine, or lysine residues (26, 27). This suggests a possible coordination of auxiliary cluster I by three cysteine residues and a non-cysteine ligand (27) in these enzymes. Phylogenetic analysis revealed that the KW_

Catalysis of C–C bond by a SPASM domain radical SAM enzyme

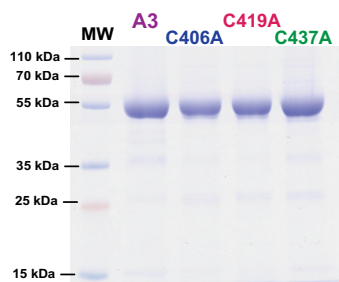
a



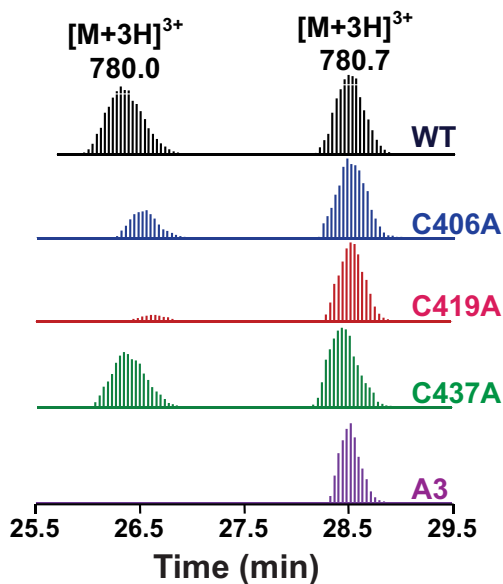
b



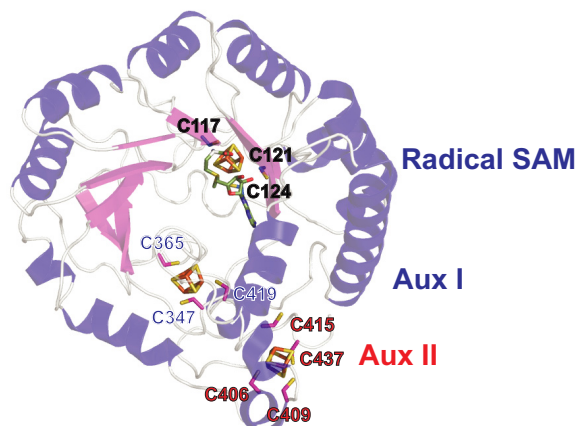
d



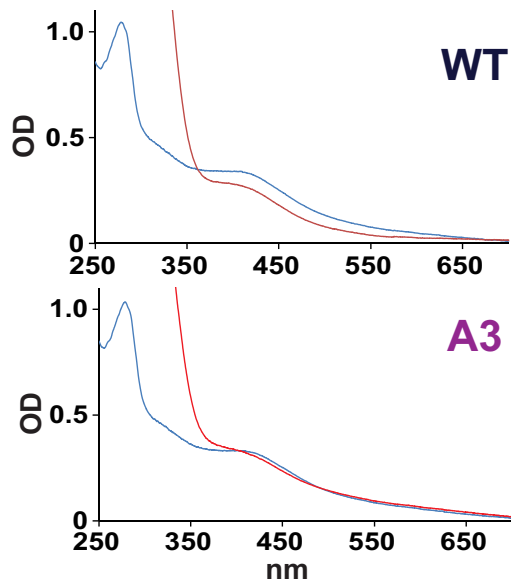
f



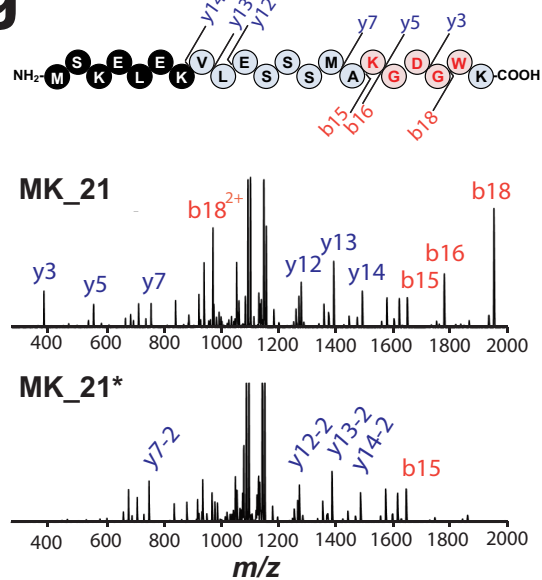
c



e



g



cyclase clustered with anSME and three enzymes catalyzing thioether bond formation, including AlbA, whose SPASM domain has been shown recently to contain two [4Fe-4S] clusters (Fig. 4*b*).

To probe the function of these cysteine residues, we built a structural model for the KW_cyclase (Fig. 4*c*) using the I-Tasser server (28). The model predicted the coordination of auxiliary cluster II by Cys-406, Cys-409, Cys-415, and Cys-437. This model also disclosed that Cys-347, Cys-365, and Cys-419 are perfectly positioned to coordinate auxiliary cluster I (Fig. 4*c*), as suggested by sequence alignment (Fig. 4*a*). To probe for the existence of this cluster, we constructed three Cys-to-Ala single mutants: C406A, C419A, and C437A. We also constructed a triple mutant (A3) in which the residues Cys-117, Cys-121, and Cys-124, predicted to coordinate the radical SAM [4Fe-4S] cluster, were mutated to alanine. All mutants were successfully purified (Fig. 4*d*), and, after anaerobic reconstitution, their UV-visible spectra were recorded (supplemental Fig. S8). The three single Cys-to-Ala mutants had UV spectra and iron-sulfur contents ($85\% \pm 17\%$) comparable with the wild-type enzyme. The A3 mutant contained 11.6 ± 0.2 mol of iron and 14.0 ± 0.3 mol of sulfide per mole of protein, suggesting the presence of more than one [4Fe-4S] cluster.

Upon addition of sodium dithionite, the UV-visible absorption spectrum of the wild-type enzyme showed a decrease in absorbance in the 420- to 600-nm region ($\sim 20\%$), consistent with the presence of one redox-active [4Fe-4S] cluster (Fig. 4*e*). In contrast, under similar conditions, the UV-visible spectrum of the A3 mutant exhibited no significant change, indicating that it contains no [4Fe-4S] cluster reducible under these conditions (Fig. 4*e*).

We further assayed the activity of the four mutants against the MK_21 peptide. As expected, the A3 mutant was unable to cleave SAM and did not lead to formation of any peptide product (Fig. 4*f*), demonstrating the role of Cys-117, Cys-121, and Cys-124 in the coordination of the radical SAM cluster. In contrast, the three single Cys-to-Ala mutants were able to reductively cleave SAM and to produce cyclic peptide, albeit at various levels (Figs. 4, *f* and *g*, and supplemental Fig. S9). The C437A mutant exhibited activity similar to the WT enzyme, whereas the C406A (mutated in the Auxiliary cluster II) and C419A (mutated in the Auxiliary cluster I) mutants exhibited very low levels of activity. Careful HPLC and LC/MS analyses failed to evidence the formation of any additional peptide products that could have accounted for reaction intermediates.

Collectively, these results show that, in addition to Cys-409 and Cys-415, Cys-406, Cys-419, and Cys-437 are not only conserved across SPASM domain radical SAM enzymes but that they are also important for enzyme activity, supporting their involvement in the coordination of two SPASM domain [4Fe-4S] clusters.

Discussion

SPASM domain radical SAM enzymes are emerging as a major class within the radical SAM enzyme superfamily. Until now, all SPASM domain radical SAM enzymes identified have been shown to be involved in protein or peptide post-translational modifications (Fig. 1) (7, 14, 15, 21). They have been reported to catalyze C_β (e.g. anSME (14) and KW_cyclase (8)) and C_α H atom abstraction (e.g. AlbA (6)), and they are predicted to catalyze C_γ H atom abstraction (e.g. QhpD (29) and PqqE). Interestingly, if they all catalyze the loss of two H atoms, these enzymes lead to different transformations, including amino acid oxidation and thioether and carbon-carbon bond formations (Fig. 1).

The initial step of these reactions is the reductive cleavage of SAM and the radical abstraction of an amino acid H atom. However, the next steps are not well understood. For anSME and AlbA, following H atom abstraction, the radical intermediate is further oxidized to a thioaldehyde (11, 14, 15) or an *N*-acyliminium ion (6) reaction intermediate, respectively. In the case of the KW_cyclase and PqqE, the most logical pathway implies radical addition to an aromatic residue, leading to the formation of a carbon-carbon bond.

Our study supports that the KW_cyclase is strictly specific for the Lys and Trp residues and cannot perform the cyclization reaction when these residues are mutated. We also show that this enzyme is not active on a peptide lacking the first eight amino acid residues, demonstrating that it requires an intact leader peptide for activity in contrast to other SPASM domain radical SAM enzymes (6, 14, 15, 30). Interestingly, in the ME_30 peptide (Fig. 2*c*), the KGDGW motif is duplicated, but this second motif is never modified, as demonstrated by the absence of activity on the peptide variants (Fig. 2*f*). The function of the leader peptide is thus likely to correctly position the peptide within the enzyme active site.

We also proved that the core sequence, composed of 21 residues, is an efficient substrate. Interestingly, this sequence is present in the human pathogen *S. agalactiae*, suggesting that this peptide might be produced by this bacterium and likely

Figure 4. Investigation of the [4Fe-4S] clusters present in KW_cyclase. *a*, sequence alignment of the conserved cysteine residues present in KW_cyclase (KW_C), anSME, AlbA, PqqE, and MftC. The cysteine residues involved in the coordination of auxiliary cluster I (Aux I) and II (Aux II), according to the anSME structure, are highlighted in blue and red, respectively. Residues conserved among at least three sequences are highlighted in black. Amino acids occupying the position of Cys-261 (in anSME) are highlighted in gray. *b*, molecular phylogenetic analysis of representative SPASM domain radical SAM enzymes: KW_cyclase, anSME, AlbA, PqqE, and MftC. The evolutionary history was inferred by using the maximum likelihood method. The percentage of replicate trees in which the associated taxa clustered together in the bootstrap test is indicated next to the branches (1000 replicates). The SPASM domain radical SAM enzymes catalyzing protein modifications are highlighted in blue. SPASM domain radical SAM enzymes catalyzing thioether bond formation on peptides are highlighted in green. *c*, structural model of the KW_cyclase. SAM is depicted in green and colored by atom elements. Cysteine residues predicted to be involved in the coordination of the radical SAM [4Fe-4S] (Cys-117, Cys-121, and Cys-124) and the coordination of the auxiliary cluster I (Cys-347, Cys-365, and Cys-419) and auxiliary cluster II (Cys-406, Cys-409, Cys-415, and Cys-437) are indicated. *d*, gel electrophoresis analysis (SDS-PAGE, 12.5%) of the purified A3, C437A, C419A, and C406A mutants. MW, molecular weight. *e*, UV-visible spectrum of the wild-type (10 μ M, top traces) and the A3 mutant (10 μ M, bottom trace) before (blue traces) and after (red traces) 20-min incubation with sodium dithionite. OD, optical density. *f*, LC/MS analysis of the peptide MK_21 incubated with the WT or the A3, C437A, C419A, or C406A mutants. Reactions were performed by incubating the respective proteins (50 μ M) after anaerobic reconstitution with the MK_21 peptide substrate (1 mM), SAM (1 mM), DTT (3 mM), and sodium dithionite (2 mM) for 2 h. *g*, LC/MS-MS analysis of the MK_21 peptide and the cyclic MK_21* peptide produced by the (WT) KW_cyclase. The characteristic ions are indicated. Similar fragmentation patterns were obtained for the C437A, C419A, and C406A mutants.

Catalysis of C–C bond by a SPASM domain radical SAM enzyme

other bacteria, including streptococci, lactococci, and even the Gram-negative bacterium *P. putida*.

Previous reports have indicated that mutation of two conserved cysteine residues, predicted to coordinate auxiliary cluster II, hinders enzyme activity. We show here that single mutation of cysteine residues involved in the coordination of auxiliary clusters II and I only reduces the activity of the enzyme. Indeed, all enzyme variants produced cyclic peptides *in vitro*, except the enzyme lacking the radical SAM cluster (mutant A3). Intriguingly, among the SPASM domain radical SAM enzymes characterized to date, only anSME possesses eight conserved cysteine residues in its SPASM domain (11, 20), which are involved in the coordination of two [4Fe-4S] clusters. In the recently discovered SPASM domain enzymes (*i.e.* AlbA, ThnB, QhpD, MtfC, and KW_cyclase), and possibly in the most distantly related PqqE enzyme (11), seven cysteine residues are strictly conserved with anSME (Fig. 4a). Interestingly, all of these SPASM domain radical SAM enzymes lack the same cysteine residue, which corresponds to Cys-261, involved in the coordination of auxiliary cluster I in anSME (11, 19). It is very unlikely that all of these enzymes have conserved the auxiliary cluster II and lost the auxiliary cluster I, which is the most buried one, in close proximity with the radical SAM cluster and likely to interact with the substrates of the respective enzymes (either directly or indirectly). Conversely, it is striking that three of four cysteine residues are conserved in these enzymes despite sharing no significant sequence homologies. Our data support that these novel SPASM domain radical SAM enzymes likely coordinate the auxiliary cluster I using three cysteine residues and a non-cysteine ligand. Recent examples of such a type of coordination have been found in the radical SAM enzyme lipoyl synthase (26, 31) and in several other iron-sulfur proteins.

These non-cysteine ligands could be used by SPASM domain radical SAM enzymes to finely tune the redox properties of the [4Fe-4S] clusters, as shown for fumarate reductase (32) or glutaredoxins (33). However, after AlbA (6) and now the KW_cyclase, it is likely that a growing number of SPASM domain radical SAM enzymes will exhibit a similar type of [4Fe-4S] cluster coordination. Further studies will undoubtedly explain why nature evolved such a sophisticated control of iron-sulfur clusters and their reactivity.

Experimental procedures

Cloning, expression, and enzyme purification

The gene *ster_1356* coding for the KW_cyclase from *S. thermophilus* LMD-9 was synthesized by Life Technologies and expressed as a Strep-tag fusion protein using a pASK plasmid. The gene construct was verified by sequencing. The construct was transformed in *E. coli* BL21 (DE3) for protein expression. Transformed *E. coli* was grown in Luria-Bertani medium using the following conditions. The growth medium was supplemented with ampicillin (100 $\mu\text{g ml}^{-1}$), and bacterial growth was performed at 37 °C until $A_{600\text{ nm}}$ reached 0.6. The expression of the *Ster_1356* protein was induced by adding anhydrotetracycline (200 nM final concentration) to the cells, and protein expression was performed during 18 h at 20 °C. Cells were harvested by centrifugation and resuspended in Tris-HCl

buffer (pH 7.5) (buffer A: 50 mM Tris and 300 mM KCl). Cells were disrupted by sonication in the presence of 1% (v/v) Triton X-100 and 1% (v/v) 2-mercaptoethanol, and the supernatant was collected after centrifugation at 45,000 $\times g$ during 1 h. Protein purification was done on a Strep-Tactin column equilibrated with buffer A, and the protein was eluted with 1 mM desthiobiotin in the presence of 3 mM dithiothreitol in buffer A. The protein was concentrated and stored at –80 °C. The genes encoding the protein variants C406A, C419A, C437A, and C117A/C121A/C124A were synthesized by Life Technologies. These genes were expressed, and the proteins were purified similarly as the wild-type enzyme.

Enzymatic assays

The peptides used in this study were ordered from Proteogenix with a purity of >98%. For [Fe-S] cluster reconstitution, proteins were incubated for 12 h at 6 °C in the presence of 3 mM DTT with a 10-fold molar excess of $(\text{NH}_4)_2\text{Fe}(\text{SO}_4)_2$ (Sigma-Aldrich) and Na_2S (Sigma-Aldrich). The proteins were desalted on a PD-10 column and concentrated.

Enzymatic assays contained 50 μM reconstituted protein, 1 mM SAM, 3 mM DTT, 1 mM peptide, and 2 mM sodium dithionite unless otherwise indicated. Samples were incubated at 20 °C under anaerobic and reducing conditions. Kinetic analyses were performed in triplicate.

HPLC analysis

HPLC analysis was carried out on an Agilent 1200 series Infinity chromatographic system. Samples were diluted 1:10 in H_2O containing 0.1% (v/v) TFA. A reverse-phase column (LiChroCART RP-18e, 5 μm) was equilibrated with 100% solvent A (H_2O , 0.1% (v/v) TFA). The gradient of 1.2%/min was applied using solvent B (80% (v/v) CH_3CN , 0.1% TFA) and a flow rate of 1 ml/min.

LC/MS-MS analysis

Peptide mass analyses were realized on a MALDI-TOF mass spectrometer (Voyager DEstr, Applied Biosystems) in reflector mode with α -cyano-4-hydroxycinnamic acid as a matrix. Peptide fragmentation analyses were realized by coupling liquid chromatography to mass spectrometry using an Ultimate 3000 LC system (Dionex) connected to an LTQ or Qexactive mass spectrometer (Thermo Scientific) in positive mode with a nano-electrospray ion source. The samples were diluted 100 times in formic acid 0.1% (v/v). 1 μl of sample was directly injected onto Pepmap100 C18 (0.075 \times 15 cm, 100 Å, 3 μm) and eluted by a linear gradient of 2% (v/v)/min of mobile phase B (80% (v/v) CH_3CN , 20% H_2O , 0.1% formic acid) during 25 min at a flow rate of 300 nl min^{-1} . The doubly charged ion corresponding to peptides MK21, MK21*, VK14, and VK14* were selected for fragmentation by collision-induced dissociation or higher-energy collisional dissociation in the linear ion trap or in the Ctrap with a normalized collision energy fixed to 35%.

NMR spectroscopy

The freeze-dried linear and cyclic 14-amino acid samples were dissolved in 120 μl of D_2O (99.96%) and transferred into

3-mm NMR sample tubes. The NMR spectra were recorded on a Bruker AVANCETM III 600-MHz spectrometer using a 5-mm ¹H/¹³C/¹⁵N/³¹P cryoprobe equipped with a z gradient. The optimum temperature at which there was no overlap of the water signal with signals from the amino acids was 278 K. The residual HOD signal was used as reference (δ_{H} 4.9955 at 278 K) for ¹H chemical shifts. The assignments of ¹H and ¹³C resonances were obtained from ¹H-¹H COSY, TOCSY, and NOESY and from ¹H-¹³C multiplicity-edited HSQC and HMBC experiments from the Bruker pulse sequence library. A mixing time of 120 ms was used for TOCSY and 100 and 500 ms for NOESY experiments. For assignment of NH resonances and establishment of the peptide sequence, the cyclic peptide sample was dissolved in 60% D₂O/40% H₂O. The TOCSY and NOESY spectra were obtained at 278 K as for D₂O solutions.

Protein structure prediction of KW_cyclase

The structural model was built using I-Tasser (28). The best identified structural analog in the PDB was anSME (PDB code 4K36). We generated a model of KW_cyclase encompassing residues 103–337 and anSME (PDB code 4K36) as a template.

Iron and sulfide titration

Determination of the iron and sulfide content of the protein samples was performed as follows. For iron titration, 100 μ l of 5 μ M enzyme was mixed with 100 μ l of HCl 1% (v/v) and incubated at 80 °C for 10 min. Tubes were allowed to cool down at room temperature prior to sequential addition of 500 μ l of 7.5% ammonium acetate, 100 μ l of 4% (w/v) ascorbic acid, and 100 μ l of 2.5% (w/v) SDS. Iron chelation was achieved by adding 100 μ l of 1.5% Ferene (w/v), followed by 10-min centrifugation at 13,000 \times g. The (Ferene)₃-Fe(II) complex absorbance was recorded at 593 nm ($\epsilon = 33.5 \text{ mM}^{-1} \text{ cm}^{-1}$).

For sulfide titration, 200 μ l of 5 μ M enzyme was mixed with 600 μ l of 1% (w/v) zinc acetate and 50 μ l of 7% (v/v) NaOH. Simultaneous addition of 0.1% (v/v) *N,N'*-dimethyl-*p*-phenylene-diamine (DMPD) and 10 mM FeCl₃ was performed, and, after centrifugation, methylene blue absorbance was recorded at 670 nm ($\epsilon = 27.4 \text{ mM}^{-1} \text{ cm}^{-1}$).

Author contributions—A. B., L. D., A. G., P. R., X. K., C. S., and O. B. performed the experiments and analyzed the data. A. B. and O. B. directed the study, analyzed the data, and wrote the manuscript. All authors approved the final version of the manuscript.

References

- Broderick, J. B., Duffus, B. R., Duschene, K. S., and Shepard, E. M. (2014) Radical *S*-adenosylmethionine enzymes. *Chem. Rev.* **114**, 4229–4317
- Mehta, A. P., Abdelwahed, S. H., Mahanta, N., Fedoseyenko, D., Philmus, B., Cooper, L. E., Liu, Y., Jhulki, I., Ealick, S. E., and Begley, T. P. (2015) Radical *S*-adenosylmethionine (SAM) enzymes in cofactor biosynthesis: a treasure trove of complex organic radical rearrangement reactions. *J. Biol. Chem.* **290**, 3980–3986
- Benjdia, A., and Berteau, O. (2016) Sulfatases and radical SAM enzymes: emerging themes in glycosaminoglycan metabolism and the human microbiota. *Biochem. Soc. Trans.* **44**, 109–115
- Berteau, O., and Benjdia, A. (2017) DNA repair by the radical SAM enzyme spore photoproduct lyase: from biochemistry to structural investigations. *Photochem. Photobiol.* **93**, 67–77
- Arnison, P. G., Bibb, M. J., Bierbaum, G., Bowers, A. A., Bugni, T. S., Bulaj, G., Camarero, J. A., Campopiano, D. J., Challis, G. L., Clardy, J., Cotter, P. D., Craik, D. J., Dawson, M., Dittmann, E., Donadio, S., *et al.* (2013) Ribosomally synthesized and post-translationally modified peptide natural products: overview and recommendations for a universal nomenclature. *Nat. Prod. Rep.* **30**, 108–160
- Benjdia, A., Guillot, A., Lefranc, B., Vaudry, H., Leprince, J., and Berteau, O. (2016) Thioether bond formation by SPASM domain radical SAM enzymes: $\text{C}\alpha$ H-atom abstraction in subtilisin A biosynthesis. *Chem. Commun. (Camb.)* **52**, 6249–6252
- Flühe, L., Knappe, T. A., Gattner, M. J., Schäfer, A., Burghaus, O., Linne, U., and Marahiel, M. A. (2012) The radical SAM enzyme AlbA catalyzes thioether bond formation in subtilisin A. *Nat. Chem. Biol.* **8**, 350–357
- Schramma, K. R., Bushin, L. B., and Seyedsayamdost, M. R. (2015) Structure and biosynthesis of a macrocyclic peptide containing an unprecedented lysine-to-tryptophan crosslink. *Nat. Chem.* **7**, 431–437
- Parent, A., Guillot, A., Benjdia, A., Chartier, G., Leprince, J., and Berteau, O. (2016) The B12-radical SAM enzyme PoyC catalyzes valine C- β -methylation during polytheonamide biosynthesis. *J. Am. Chem. Soc.* **138**, 15515–15518
- Pierre, S., Guillot, A., Benjdia, A., Sandström, C., Langella, P., and Berteau, O. (2012) Thiostrepton tryptophan methyltransferase expands the chemistry of radical SAM enzymes. *Nat. Chem. Biol.* **8**, 957–959
- Benjdia, A., Subramanian, S., Leprince, J., Vaudry, H., Johnson, M. K., and Berteau, O. (2010) Anaerobic sulfatase-maturing enzyme: a mechanistic link with glycyl radical-activating enzymes? *FEBS J.* **277**, 1906–1920
- Haft, D. H., and Basu, M. K. (2011) Biological systems discovery in silico: radical *S*-adenosylmethionine protein families and their target peptides for posttranslational modification. *J. Bacteriol.* **193**, 2745–2755
- Barr, I., Latham, J. A., Iavarone, A. T., Chantarojsiri, T., Hwang, J. D., and Klinman, J. P. (2016) Demonstration that the radical *S*-adenosylmethionine (SAM) enzyme PqqE catalyzes *de novo* carbon-carbon cross-linking within a peptide substrate PqqA in the presence of the peptide chaperone PqqD. *J. Biol. Chem.* **291**, 8877–8884
- Benjdia, A., Leprince, J., Sandström, C., Vaudry, H., and Berteau, O. (2009) Mechanistic investigations of anaerobic sulfatase-maturing enzyme: direct C β H-atom abstraction catalyzed by a radical AdoMet enzyme. *J. Am. Chem. Soc.* **131**, 8348–8349
- Benjdia, A., Leprince, J., Guillot, A., Vaudry, H., Rabot, S., and Berteau, O. (2007) Anaerobic sulfatase-maturing enzymes: radical SAM enzymes able to catalyze *in vitro* sulfatase post-translational modification. *J. Am. Chem. Soc.* **129**, 3462–3463
- Berteau, O., Guillot, A., Benjdia, A., and Rabot, S. (2006) A new type of bacterial sulfatase reveals a novel maturation pathway in prokaryotes. *J. Biol. Chem.* **281**, 22464–22470
- Bruender, N. A., and Bandarian, V. (2016) The radical *S*-adenosyl-L-methionine enzyme MftC catalyzes an oxidative decarboxylation of the C terminus of the MftA peptide. *Biochemistry* **55**, 2813–2816
- Benjdia, A., Martens, E. C., Gordon, J. I., and Berteau, O. (2011) Sulfatases and a radical *S*-adenosyl-L-methionine (AdoMet) enzyme are key for mucosal foraging and fitness of the prominent human gut symbiont *Bacteroides thetaiotaomicron*. *J. Biol. Chem.* **286**, 25973–25982
- Benjdia, A., Subramanian, S., Leprince, J., Vaudry, H., Johnson, M. K., and Berteau, O. (2008) Anaerobic sulfatase-maturing enzymes: first dual substrate radical *S*-adenosylmethionine enzymes. *J. Biol. Chem.* **283**, 17815–17826
- Goldman, P. J., Grove, T. L., Sites, L. A., McLaughlin, M. I., Booker, S. J., and Drennan, C. L. (2013) X-ray structure of an AdoMet radical activase reveals an anaerobic solution for formylglycine posttranslational modification. *Proc. Natl. Acad. Sci. U.S.A.* **110**, 8519–8524
- Grell, T. A., Goldman, P. J., and Drennan, C. L. (2015) SPASM and twitch domains in *S*-adenosylmethionine (SAM) radical enzymes. *J. Biol. Chem.* **290**, 3964–3971
- Benjdia, A., Dehò, G., Rabot, S., and Berteau, O. (2007) First evidences for a third sulfatase maturation system in prokaryotes from *E. coli* aslB and ydeM deletion mutants. *FEBS Lett.* **581**, 1009–1014
- Weckler, S. R., Stoll, S., Tran, H., Magnusson, O. T., Wu, S. P., King, D., Britt, R. D., and Klinman, J. P. (2009) Pyrroloquinoline quinone biogenesis:

Catalysis of C–C bond by a SPASM domain radical SAM enzyme

- demonstration that PqqE from *Klebsiella pneumoniae* is a radical *S*-adenosyl-L-methionine enzyme. *Biochemistry* **48**, 10151–10161
24. Ibrahim, M., Guillot, A., Wessner, F., Algaron, F., Besset, C., Courtin, P., Gardan, R., and Monnet, V. (2007) Control of the transcription of a short gene encoding a cyclic peptide in *Streptococcus thermophilus*: a new quorum-sensing system? *J. Bacteriol.* **189**, 8844–8854
 25. Flühe, L., Burghaus, O., Wieckowski, B. M., Giessen, T. W., Linne, U., and Marahiel, M. A. (2013) Two [4Fe-4S] clusters containing radical SAM enzyme SkfB catalyze thioether bond formation during the maturation of the sporulation killing factor. *J. Am. Chem. Soc.* **135**, 959–962
 26. Harmer, J. E., Hiscox, M. J., Dinis, P. C., Fox, S. J., Iliopoulos, A., Hussey, J. E., Sandy, J., Van Beek, F. T., Essex, J. W., and Roach, P. L. (2014) Structures of lipoyl synthase reveal a compact active site for controlling sequential sulfur insertion reactions. *Biochem. J.* **464**, 123–133
 27. Qi, W., and Cowan, J. A. (2011) Structural, mechanistic and coordination chemistry of relevance to the biosynthesis of iron-sulfur and related iron cofactors. *Coord. Chem. Rev.* **255**, 688–699
 28. Yang, J., Yan, R., Roy, A., Xu, D., Poisson, J., and Zhang, Y. (2015) The I-TASSER suite: protein structure and function prediction. *Nat. Methods* **12**, 7–8
 29. Nakai, T., Ito, H., Kobayashi, K., Takahashi, Y., Hori, H., Tsubaki, M., Tanizawa, K., and Okajima, T. (2015) The radical *S*-adenosyl-L-methionine enzyme QhpD catalyzes sequential formation of intra-protein sulfur-to-methylene carbon thioether bonds. *J. Biol. Chem.* **290**, 11144–11166
 30. Benjdia, A., Guillot, A., Ruffié, P., Leprince, J., and Berteau, O. (2017) Post-translational modification of ribosomally synthesized peptides by a radical SAM epimerase in *Bacillus subtilis*. *Nat. Chem.* **10**, 1038/nchem.2714
 31. McLaughlin, M. I., Lanz, N. D., Goldman, P. J., Lee, K. H., Booker, S. J., and Drennan, C. L. (2016) Crystallographic snapshots of sulfur insertion by lipoyl synthase. *Proc. Natl. Acad. Sci. U.S.A.* **113**, 9446–9450
 32. Cheng, V. W., Tran, Q. M., Boroumand, N., Rothery, R. A., Maklashina, E., Cecchini, G., and Weiner, J. H. (2013) A conserved lysine residue controls iron-sulfur cluster redox chemistry in *Escherichia coli* fumarate reductase. *Biochim. Biophys. Acta* **1827**, 1141–1147
 33. Li, H., Mapolelo, D. T., Dingra, N. N., Keller, G., Riggs-Gelasco, P. J., Winge, D. R., Johnson, M. K., and Outten, C. E. (2011) Histidine 103 in Fra2 is an iron-sulfur cluster ligand in the [2Fe-2S] Fra2-Grx3 complex and is required for *in vivo* iron signaling in yeast. *J. Biol. Chem.* **286**, 867–876
 34. Benjdia, A., Pierre, S., Gherasim, C., Guillot, A., Carmona, M., Amara, P., Banerjee, R., and Berteau, O. (2015) The thiostrepton A tryptophan methyltransferase TsrM catalyses a cob(II)alamin-dependent methyl transfer reaction. *Nat. Commun.* **6**, 8377